Effect of CuO as Sintering Additive in Scandium Cerium and Gadolinium-Doped Zirconia-Based Solid Oxide Electrolysis Cell for Steam Electrolysis

R. Visvanichkul [1], S. Peng-Ont [2], W. Ngampuengpis [2], N. Sirimungkalakul [2], P. Puengjinda [2], T. Jiwanuruk [2], T. Sornchamni [2] and P. Kim-Lohsoontorn [1,*]

[1] Centre of Excellence on Catalysis and Catalytic Reaction Engineering, Department of Chemical Engineering, Faculty of Engineering, Chulalongkorn University, Bangkok 10330, Thailand; r.visvanichkul@gmail.com

[2] PTT Innovation Institute, PTT Public Company Limited, Ayutthaya 13170, Thailand; saranya.p@pttplc.com (S.P.-O.); Ng.watcharin@gmail.com (W.N.); Nkanjanabat@gmail.com (N.S.); pramote.pu@pttplc.com (P.P.); tara.j@pttplc.com (T.J.); thana.s@pttplc.com (T.S.)

* Correspondence: pattaraporn.k@chula.ac.th

Abstract: The effect of CuO as a sintering additive on the electrolyte of solid oxide electrolysis cells (SOECs) was investigated. 0.5 wt% CuO was added into $Sc_{0.1}Ce_{0.05}Gd_{0.05}Zr_{0.89}O_2$ (SCGZ) electrolyte as a sintering additive. An electrolyte-supported cell (Pt/SCGZ/Pt) was fabricated. Phase formation, relative density, and electrical conductivity were investigated. The cells were sintered at 1373 K to 1673 K for 4 h. The CuO significantly affected the sinterability of SCGZ. The SCGZ with 0.5 wt% CuO achieved 95% relative density at 1573 K while the SCGZ without CuO could not be densified even at 1673 K. Phase transformation and impurity after CuO addition were not detected from XRD patterns. Electrochemical performance was evaluated at the operating temperature from 873 K to 1173 K under steam to hydrogen ratio at 70:30. Adding 0.5 wt% CuO insignificantly affected the electrochemical performance of the cell. Activation energy of conduction (E_a) was 72.34 kJ mol^{-1} and 74.93 kJ mol^{-1} for SCGZ and SCGZ with CuO, respectively.

Keywords: solid oxide electrolysis cells; sintering additive; CuO; hydrogen production; steam electrolysis

1. Introduction

Global climate change is an important issue that is clearly found to affect the environment and humanity. Greenhouse gas emission is the major cause for retaining heat in the atmosphere, leading to climate change. Greenhouse gases are mainly generated from the combustion of fossil fuel such as petroleum, natural gas, and coal. Hydrogen is the one of the promising energy carriers for better environment since only water and energy are produced from hydrogen combustion [1,2]. Moreover, hydrogen can be used as a feedstock for various industrial chemical productions [3–5].

Solid oxide electrolysis cells (SOECs) are used to produce high purity hydrogen from steam electrolysis reaction at elevated temperatures. Material selection is one of the challenges faced in the implementation of SOEC. The operation may operate under severe condition in the production scale. Sealant of gas leakage between the stack needs to be modified [6]. Material choice for SOEC electrode is often similar to solid oxide fuel cell [7–9]. Therefore, 8 mol% yttria stabilized zirconia (YSZ), which is a conventional electrolyte in solid oxide fuel cell [10–13], is generally used as the SOEC electrolyte. Attempt has been made to seek for fast ionic conductor instead of conventional YSZ [14–18]. Doped-cerate- or doped-zirconia-based electrolyte has been studied. Scandium oxide (Sc_2O_3) is the one among the dopants for zirconia-based electrolyte (Scandium stabilized zirconia, ScSZ) that improves the ionic conductivity when compared with YSZ electrolyte. Similar ionic radius

between Sc^{3+} and Zr^{4+} can cause low internal stress and the activation energy of conduction [16]. However, phase transition can occur in ScSZ electrolyte, leading to loss of conductivity. Abbas et al. [19] prepared co-doping of 1 mol% Gd_2O_3, CaO, and CeO_2 with 10 mol% Sc_2O_3 into zirconia structure to reduce phase transition and it was found that 1 mol% CeO_2 and 10 mol% Sc_2O_3 as dopants provide relatively highest conductivity, likely because of the close ionic radius of Ce^{4+} and Zr^{4+} compared to other dopants. Shin et al. [20] investigated the co-doping of trivalent oxides (Gd_2O_3, Yb_2O_3, and Y_2O_3) with CeO_2 into scandium stabilized zirconia structure. It was reported that co-doping of Gd_2O_3 with CeO_2 provides relatively higher ionic conductivity when compared with other oxides. However, doped-zirconia electrolyte often requires relatively high sintering temperature (~1723 K) for electrolyte densification. High sintering temperature of the electrolyte can lead to degradation issue in other cell compartments, leading to difficulty in fabrication process. For example, in electrode-supported cells, nickel (Ni) component in an electrode can agglomerate at high temperature, leading to decreasing three phase boundary of the electrode. In metal-supported cell, metal part (often containing iron (Fe) or Ni content) cannot withstand high sintering temperature because of a large thermal expansion coefficient of the metal. Therefore, lower sintering temperature for electrolyte is required to enhance the fabrication process of the cell.

Sintering additive can promote densification and help reduce sintering temperature of the electrolyte. The additive can melt to form liquid phase during the sintering process. Solid grain of the electrolyte is wet by liquid phase which provide capillary force pulling the grain denser [16]. There are varied metal oxide such as CuO, NiO, Fe_2O_3, and MnO_2 that have been used as sintering additives for zirconia-based electrolyte [21–24]. However, adding sintering additives which are often metal oxides can induce electronic conductivity in the electrolyte. Myung et al. [25] investigated scanning electron microscope (SEM) images of sintered YSZ by varying amount of CuO additive from 0 to 1.5 wt%. It was found that optimum quantity of additive and sintering temperature was 0.5 wt% of CuO and 1623 K, respectively. Our previous work [26] reported other metal oxides (NiO, Co_2O_3, and ZnO) as additives in barium cerate-based electrolyte. The additives helped increase sinterability of the electrolyte and provided different conductivity for the electrolyte.

In this research, $Sc_{0.1}Ce_{0.05}Gd_{0.05}Zr_{0.89}O_2$ (SCGZ) was used as an electrolyte in SOEC. CuO was added into the electrolyte as a sintering additive. The effect of sintering additive on phase formation, cell densification, and electrical performance were investigated.

2. Experimental

2.1. Cell Fabrication

Scandium cerium- and gadolinium-doped zirconia ($Sc_{0.1}Ce_{0.05}Gd_{0.05}Zr_{0.89}O_2$, SCGZ) was fabricated into an electrolyte-supported SOEC. Three grams of SCGZ powder (Kceracell, Chungcheongnam-do, Republic of Korea) were pressed at 24 MPa into a pellet with diameter of 25 mm and thickness of 1.4 mm. The pellets were then sintered at 1373 K to 1673 K for 4 h. The electrolyte pellet with sintering additive was fabricated using the same method when 0.5 wt% CuO was added into the SCGZ staring powder. The relative density of the sintered electrolyte pellet was calculated following Equation (1).

$$\text{Relative density} = \frac{\text{Actual density}}{\text{Theoretical density}} \times 100 \tag{1}$$

where actual density is the bulk density of sintered cell. The theoretical density was obtained by lattice parameter from X-ray diffraction (XRD) analysis (Bruker D8 Advance, Billerica, MA, USA).

Platinum (Pt) conductive paste (70 wt% Pt, Nexceris) was coated on the both sides of the electrolyte pellet as electrodes with thickness and area of ~30 μm and ~0.5 cm^2, respectively. The schematic of cell component was shown as Figure 1. The cell was then fired at 1173 K for 2 h. It should be noted that the choices of electrode used depend on the deposition technique, the operating temperature, and the type

of conductivity. Using gold or platinum as working electrode was reported to perform well at high temperature but below 873 K they are relatively blocking oxygen [27].
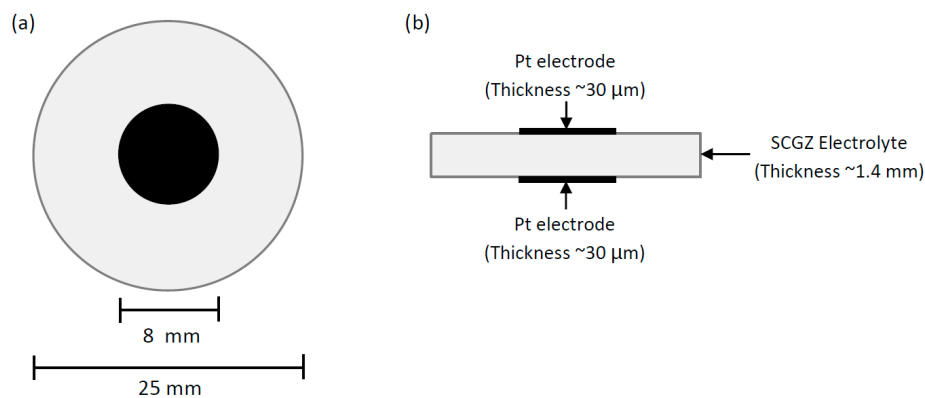
Figure 1. Schematic drawing of electrolyte-supported solid oxide electrolysis cells (SOEC); (**a**) top view, (**b**) side view.

2.2. Characterization

Phase and crystallite size of sintered electrolyte were determined using XRD with CuKα source (Bruker D8 Advance, Billerica, MA, USA). The microstructure of the samples was investigated using SEM (Hitachi S-3400N JEOL model S-3400, Tokyo, Japan). The average grain sizes were calculated by linear intersection method.

2.3. Electrochemical Performance Measurement

Electrochemical performance was measured in a controlled temperature from 873 K to 1173 K with the feed containing steam and hydrogen at the ratio of 70:30. The fabricated cell was attached with Pt mesh and wire (Kceracell, Chungcheongnam-do, Korea) for electrical connection. The cell was placed on a cell holder with high temperature sealant (Ceramabond 552, Aramco, Houston, TX, USA). The holder was installed inside a vertical furnace (Chavachote, Bangkok, Thailand). High performance liquid chromatography (HPLC) liquid pump (Teledyne SSI, State College, PA, USA) was used to supply deionized water through a heated-pipe for steam generation in the system. Linear sweep voltammetry procedure was applied to generate current/voltage (I/V) curves by controlling the potential from 0.4 V to 1.8 V with a scan rate of 20 mVs^{-1} (Metrohm Autolab, Utrecht, The Netherlands).

Resistance was determined by the slope of current/voltage (I/V) curves and the conductivity of fabricated cell (σ) was then calculated using Equation (2).

$$\sigma = L/RA \tag{2}$$

where σ is the conductivity (S cm^{-1}); L is the thickness of fabricated cell (cm); R is the cell resistance (Ω); and, A is the area of electrode (cm^2).

The activation energy of conduction (E_a) was obtained by using Arrhenius, Equation (3) with conductivity value as mentioned above.

$$\sigma T = A \cdot \exp\left(-\frac{E_a}{RT}\right) \tag{3}$$

where σ is the conductivity (S cm^{-1}); T is the absolute temperature (K); A is a constant; E_a is the activation energy of conduction (J mol^{-1}); and R is the gas constant (8.314 J K^{-1} mol^{-1}). It should be noted that the activation energy of conduction in this study was calculated from I/V curves ranging from open circuit voltage to 1.8 V. The slope of I/V curve is total resistance, which includes electrode resistance. The I/V slope was not constant and was derived using a linear regression with R-squared

(R^2) ranging from 0.90–0.97. In this study, Pt was applied as both electrodes (Pt/Electrolyte/Pt) and was expected to provide rather low resistance at operating conditions.

3. Results and Discussion

3.1. Densification of the Fabricated Cell

SEM images of SCGZ electrolyte with and without 0.5 wt% CuO sintered at varied temperature from 1423 K to 1673 K are presented in Figures 2 and 3, respectively. The microstructure images reveal that the SCGZ without the sintering additive could not be densified although high sintering temperature was used. Porosity were observed all over the SCGZ without the sintering additive. Grain boundary was observed from 1623 K but the grain size was rather small. The porosity decreased when the sintering temperature was increased. However, the relative density of the SCGZ without the sintering additive was only <90%, although high sintering temperature was increased up to 1673 K. On the other hand, densification and larger grain size were observed in the sample with the sintering additive. The grain growth was observed when increasing sintering temperature (Table 1). The added CuO could diffuse along the grain boundary and substituted in the vacancy position of the microstructure. Myung et al. [25] investigated CuO (0.3 wt% to 1.5 wt%) as sintering additive in yttria-stabilized zirconia (YSZ) sintering between 1423 K to 1673 K. It was reported that 0.5 wt% of CuO is the optimal amount providing the highest densification. Amount of optimal CuO additive at 0.5 wt% was the same for YSZ and SCGZ, likely because both materials are zirconia-based electrolyte. However, although having same optimal CuO amount, YSZ requires relatively higher sintering temperature (1623 K) when compared with SCGZ (1573 K) at the same sintering additive amount.
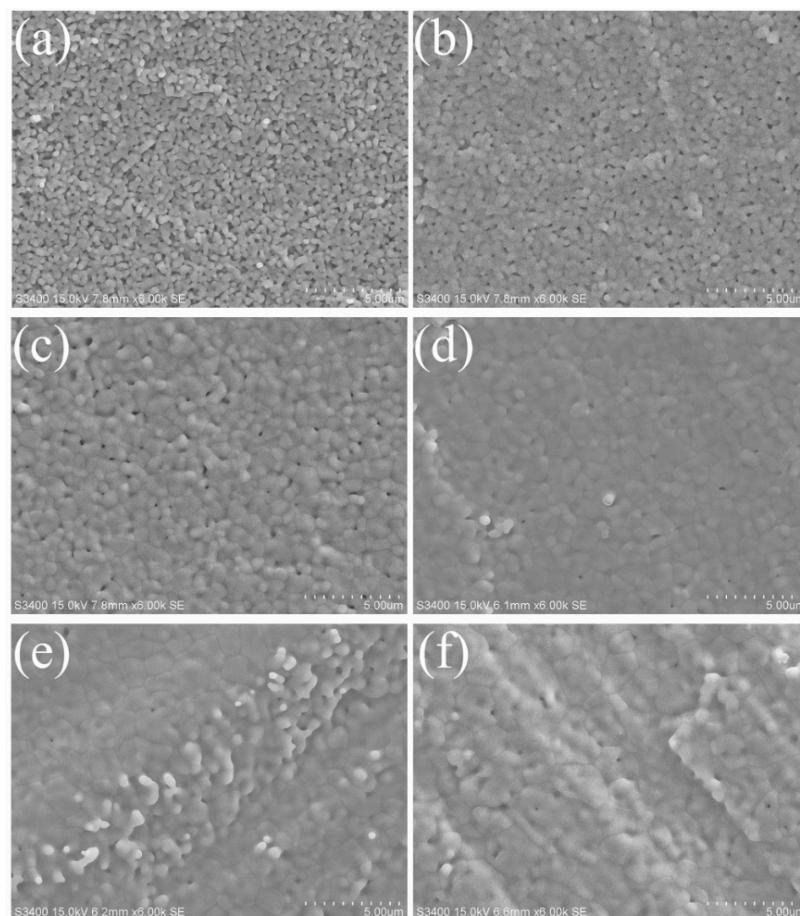
Figure 2. Scanning electron microscope (SEM) images of sintered $Sc_{0.1}Ce_{0.05}Gd_{0.05}Zr_{0.89}O_2$ (SCGZ) at (**a**) 1423 K, (**b**) 1473 K, (**c**) 1523 K, (**d**) 1573 K, (**e**) 1623 K, and (**f**) 1673 K.
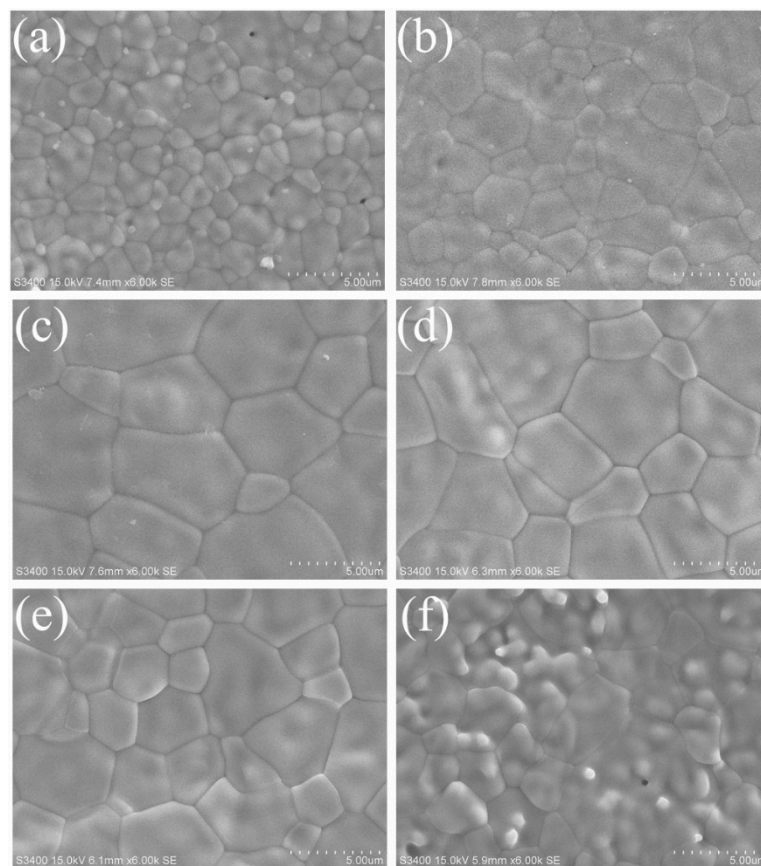
Figure 3. SEM images of sintered SCGZ with 0.5 wt% CuO at (**a**) 1423 K, (**b**) 1473 K, (**c**) 1523 K, (**d**) 1573 K, (**e**) 1623 K and (**f**) 1673 K.

Table 1. Average grain size of sinterted $Sc_{0.1}Ce_{0.05}Gd_{0.05}Zr_{0.89}O_2$ (SCGZ) electrolyte and sintered SCGZ electrolyte with 0.5 wt% CuO when sintering temperature was varied.

Sintering Temperature (K)	Average Grain Size (µm)	
	SCGZ	SCGZ with 0.5 wt% CuO
1423	-	1.58
1473	-	2.66
1523	1.04	5.02
1573	1.20	5.11
1623	1.51	3.32
1673	2.28	3.77

Adding 0.5 wt% CuO enhanced the densification of SCGZ. The relative densities of the fabricated cells are presented in Figure 4. The SCGZ without sintering additive provided rather low relative density (<90%) at all sintering temperatures, corresponding to porosity observed in the SEM images. The SCGZ with 0.5 wt% CuO could be densified at lower sintering temperature. Increasing sintering temperature from 1423 to 1673 K could help increase the relative density of the fabricated cell. The cell was densified at 95% relative density at 1573 K respect to other sintering temperature. It was reported that CuO exhibit relatively low melting point (around 1599 K) and can enhance sintering by pore filling during liquid phase sintering [28]. Increasing temperature above 1623 K was found to decrease the relative density of the fabricated cell, likely relating to the liquid phase sintering. Liou et al. [29] studied the effect of CuO as sintering additives on $CaTiO_3$ perovskite ceramics. Liquid phase sintering at grain boundary is found at sintered sample at 1723 K for 6 h and increases significantly when

increasing sintering temperature to 1743 K. However, liquid phase did not occur when increasing sintering temperature up to 1773 K for 6 h, leading to less densification. Moreover, when sintering soak time was increased to 8 h at 1723 K, liquid phase sintering significantly increases when compared with 6 h. A proper sintering temperature and soak time are important factors affecting the densification of the sample.
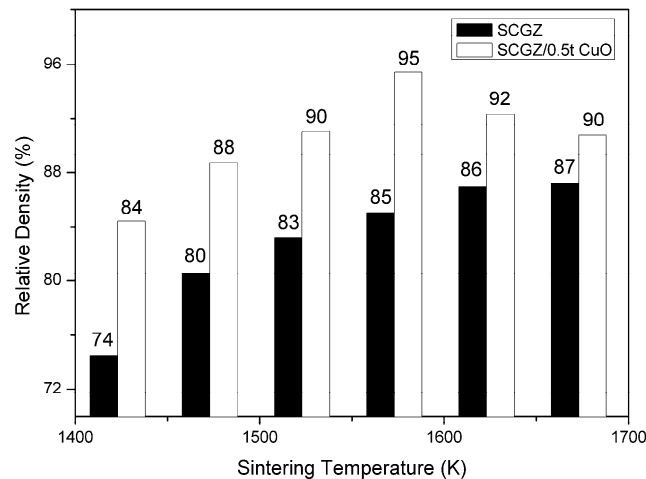
Figure 4. Relative density (%) of the SCGZ pellet and the SCGZ pellet with 0.5 wt% CuO when the sintering temperature was varied.

3.2. Phase Identification

XRD patterns of the SCGZ pellet sintered at 1673 K and the SCGZ with 0.5 wt% CuO pellet sintered at 1523 K are shown in Figure 5. The XRD patterns included main peaks at (111), (200), (220), (311), and (222) planes (COD Database ID: 1529100). Impurity phase was not detected. The XRD patterns of two samples were identical in term of the peak positions. Shifting in peaks position of the XRD patterns was not detected. This result could confirm that CuO did not form into a solid solution with SCGZ but well-mixed with SCGZ as a composite form. This results corresponded to the previous work [30]. It should be noted that CuO peaks were not detected, likely due to small amount of CuO in the sample. The average crystallite sizes were 184 nm and 202 nm for SCGZ sintered at 1673 K and SCGZ with sintering additive sintered at 1523 K, respectively, corresponding to the work that reported higher densification provided a larger grain size leading to a larger crystallite size [31].
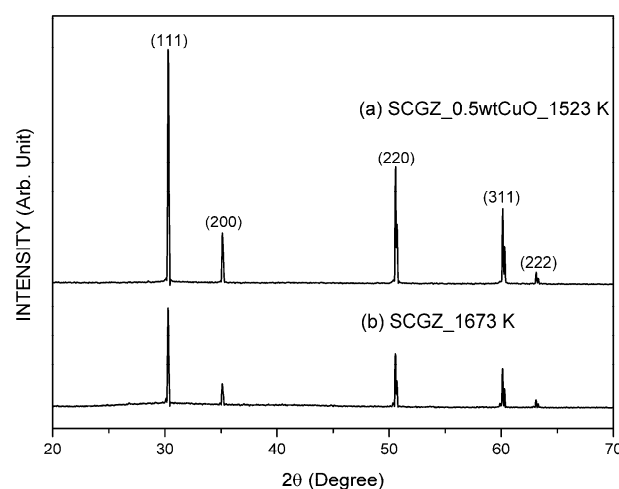
Figure 5. The X-ray diffraction patterns of (**a**) sintered SCGZ at 1673 K and (**b**) sintered SCGZ with 0.5 wt% CuO at 1523 K.

3.3. Activation Energy of Conduction

The electrochemical performance of the SOEC was evaluated. Linear sweep voltammetry was conducted from 873 K to 1173 K under a constant steam to hydrogen ratio (70:30). The I/V curves of the cells having SCGZ electrolyte without and with CuO addition are shown in Figures 6 and 7, respectively. The conductivity and activation energy of conduction are presented in Figure 8. It can be seen that the conductivity increased with increasing operating temperature. The activation energy of conduction (E_a) was 72.34 kJmol^{-1} and 74.93 kJmol^{-1} for SCGZ and SCGZ with CuO, respectively. In this study, adding 0.5 wt% CuO did not significantly affect the conductivity of the electrolyte. The use of CuO as sintering additive in various ceramic electrolytes has been reported differently. It was reported that adding CuO can lead to ionic and electrical properties modification [25,32–36]. Zhang et al. [36] found that addition of 1 wt% CuO improved the sinterability of $Sm_{0.2}Ce_{0.8}O_{1.9}$ (SDC) electrolyte. The SDC could be densified even at lower sintering temperature than 1273 K but the ionic conductivity was also decreased as a result of microstructure alteration. On the other hand, 0.5 mol% of CuO as sintering additive could provide high ionic conductivity and insignificant change in the activation energy of conduction for gadolinium-doped ceria (GDC) electrolyte [37]. In this study, 0.5 wt% CuO was used as a potential sintering additive for SCGZ electrolyte in SOEC, decreasing the sintering temperature without any significant change in the activation energy of conduction.
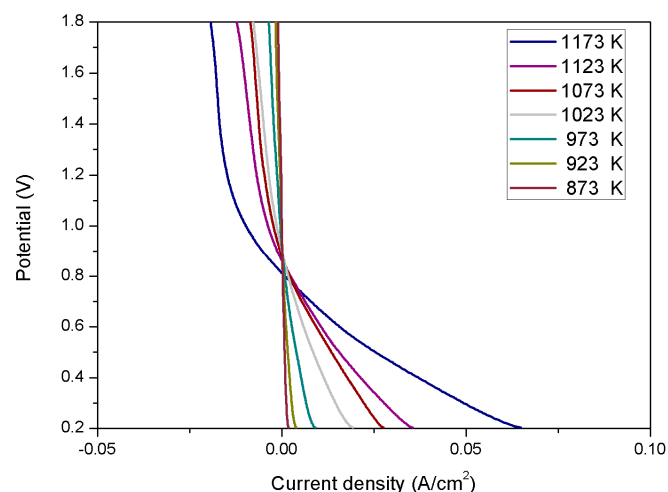
Figure 6. The I/V curves of the SCGZ electrolyte-supported SOEC conducted from 873 K to 1173 K under a constant steam to hydrogen ratio (70:30).
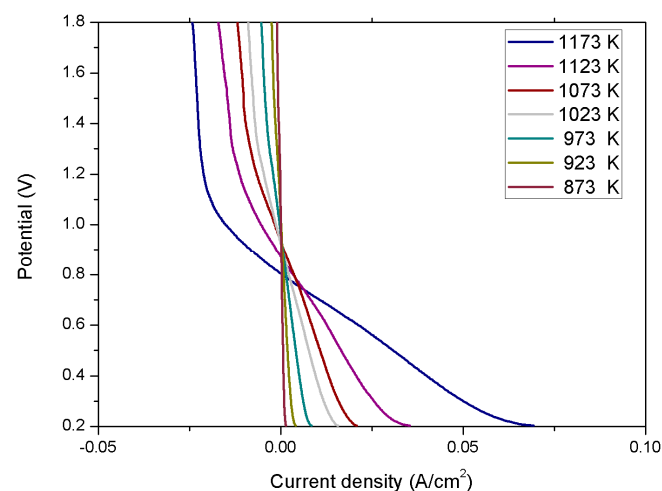
Figure 7. The I/V curves of the SCGZ with 0.5 wt% CuO electrolyte-supported SOEC conducted from 873 K to 1173 K under a constant steam to hydrogen ratio (70:30).
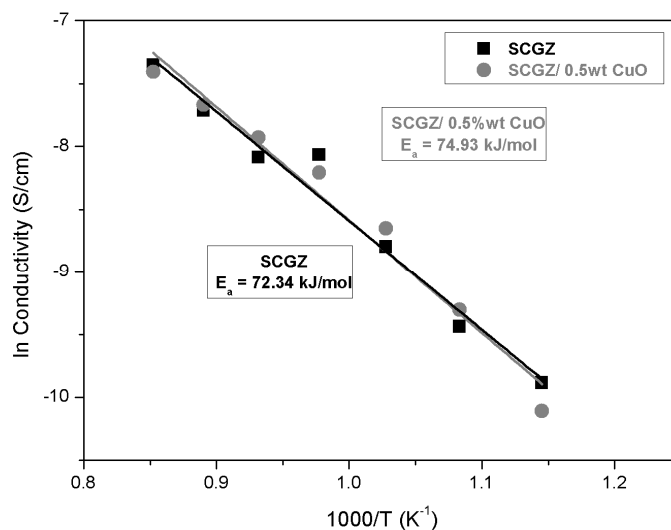
Figure 8. Activation energy of conduction (E_a) for the SOEC having SCGZ electrolyte and 0.5 wt% CuO-added SCGZ electrolyte.

4. Conclusions

0.5 wt% CuO was employed as a sintering additive for SCGZ electrolyte in SOEC. Phase formation, microstructure, relative density, and electrochemical performance of electrolyte-supported SOEC were investigated. Adding 0.5 wt% CuO helped increasing the sinterability of the electrolyte which could achieve 95% relative density with a large grain size at 1573 K. The average grain size was measured at 5.11 μm when sintering temperature was 1573 K for SCGZ with CuO. Phase transformation and impurity was not detected in the electrolyte after adding CuO. Neither peak shifting nor impurity peak were detected in the XRD patterns. Without CuO addition, the SCGZ could not be densified although sintering temperature was increased up to 1673 K. Adding CuO into SCGZ insignificantly affected the electrochemical performance of the cell. The activation energy of conduction (E_a) of the SCGZ with and without CuO was 74.93 kJ mol^{-1} and 72.34 kJ mol^{-1}, respectively.

Conflicts of Interest: The authors declare no conflict of interest.

References

1. Weng, G.-M.; Vanessa Li, C.-Y.; Chan, K.-Y. Hydrogen battery using neutralization energy. *Nano Energy* **2018**, *53*, 240–244. [CrossRef]
2. Wang, F.-C.; Hsiao, Y.-S.; Yang, Y.-Z. The Optimization of Hybrid Power Systems with Renewable Energy and Hydrogen Generation. *Energies* **2018**, *11*, 1948. [CrossRef]
3. Hawkins, A.S.; McTernan, P.M.; Lian, H.; Kelly, R.M.; Adams, M.W.W. Biological conversion of carbon dioxide and hydrogen into liquid fuels and industrial chemicals. *Curr. Opin. Biotechnol.* **2013**, *24*, 376–384. [CrossRef] [PubMed]
4. Wiesberg, I.L.; de Medeiros, J.L.; Alves, R.M.B.; Coutinho, P.L.A.; Araújo, O.Q.F. Carbon dioxide management by chemical conversion to methanol: Hydrogenation and Bi-Reforming. *Energy Convers. Manag.* **2016**, *125*, 320–335. [CrossRef]

5. Likhittaphon, S.; Panyadee, R.; Fakyam, W.; Charojrochkul, S.; Sornchamni, T.; Laosiripojana, N.; Assabumrungrat, S.; Kim-Lohsoontorn, P. Effect of CuO/ZnO catalyst preparation condition on alcohol-assisted methanol synthesis from carbon dioxide and hydrogen. *Int. J. Hydrogen Energy* **2019**, *44*, 20782–20791. [CrossRef]

6. Javed, H.; Sabato, A.G.; Herbrig, K.; Ferrero, D.; Walter, C.; Salvo, M.; Smeacetto, F. Design and characterization of novel glass-ceramic sealants for solid oxide electrolysis cell (SOEC) applications. *Int. J. Appl. Ceram. Technol.* **2018**, *15*, 999–1010. [CrossRef]

7. Kim-Lohsoontorn, P.; Kim, Y.-M.; Laosiripojana, N.; Bae, J. Gadolinium doped ceria-impregnated nickel–yttria stabilised zirconia cathode for solid oxide electrolysis cell. *Int. J. Hydrogen Energy* **2011**, *36*, 9420–9427. [CrossRef]

8. Chen, T.; Zhou, Y.; Liu, M.; Yuan, C.; Ye, X.; Zhan, Z.; Wang, S. High performance solid oxide electrolysis cell with impregnated electrodes. *Electrochem. Commun.* **2015**, *54*, 23–27. [CrossRef]

9. Kim, J.; Jun, A.; Gwon, O.; Yoo, S.; Liu, M.; Shin, J.; Lim, T.-H.; Kim, G. Hybrid-solid oxide electrolysis cell: A new strategy for efficient hydrogen production. *Nano Energy* **2018**, *44*, 121–126. [CrossRef]

10. Fernández-González, R.; Molina, T.; Savvin, S.; Moreno, R.; Makradi, A.; Núñez, P. Fabrication and electrical characterization of several YSZ tapes for SOFC applications. *Ceram. Int.* **2014**, *40*, 14253–14259. [CrossRef]

11. Talebi, T.; Sarrafi, M.H.; Haji, M.; Raissi, B.; Maghsoudipour, A. Investigation on microstructures of NiO–YSZ composite and Ni–YSZ cermet for SOFCs. *Int. J. Hydrogen Energy* **2010**, *35*, 9440–9447. [CrossRef]

12. Fondard, J.; Bertrand, P.; Billard, A.; Fourcade, S.; Batocchi, P.; Mauvy, F.; Bertrand, G.; Briois, P. Manufacturing and testing of a metal supported Ni-YSZ/YSZ/La_2NiO_4 IT-SOFC synthesized by physical surface deposition processes. *Solid State Ion.* **2017**, *310*, 10–23. [CrossRef]

13. Han, Z.; Yang, Z.; Han, M. Optimization of Ni-YSZ anodes for tubular SOFC by a novel and efficient phase inversion-impregnation approach. *J. Alloys Compd.* **2018**, *750*, 130–138. [CrossRef]

14. Yeh, T.H.; Chiang, C.M.; Lo, W.C.; Chou, C.C. Co-doping effect of divalent (Mg2+, Ca2+, Sr) and trivalent (Y3+) cations with different ionic radii on ionic conductivity of zirconia electrolytes. *J. Chin. Soc. Mech. Eng. Trans. Chin. Inst. Eng. Ser. C* **2009**, *30*, 151–158.

15. Gao, H.; Liu, J.; Chen, H.; Li, S.; He, T.; Ji, Y.; Zhang, J. The effect of Fe doping on the properties of SOFC electrolyte YSZ. *Solid State Ion.* **2008**, *179*, 1620–1624. [CrossRef]

16. Kubrin, R.; Blugan, G.; Kuebler, J. Influence of cerium doping on mechanical properties of tetragonal scandium-stabilized zirconia. *J. Eur. Ceram. Soc.* **2017**, *37*, 1651–1656. [CrossRef]

17. Vijaya Lakshmi, V.; Bauri, R. Phase formation and ionic conductivity studies on ytterbia co-doped scandia stabilized zirconia ($0.9ZrO_2$–$0.09Sc_2O_3$–$0.01Yb_2O_3$) electrolyte for SOFCs. *Solid State Sci.* **2011**, *13*, 1520–1525. [CrossRef]

18. Chen, M.; Gao, H.; Zhang, L.; Xuan, Y.; Ren, J.; Ni, M.; Lin, Z. Unlocking the nature of the co-doping effect on the ionic conductivity of CeO_2-based electrolyte. *Ceram. Int.* **2019**, *45*, 3977–3985. [CrossRef]

19. Abbas, H.A.; Argirusis, C.; Kilo, M.; Wiemhöfer, H.-D.; Hammad, F.F.; Hanafi, Z.M. Preparation and conductivity of ternary scandia-stabilised zirconia. *Solid State Ion.* **2011**, *184*, 6–9. [CrossRef]

20. Shin, H.C.; Yu, J.H.; Lim, K.T.; Lee, H.L.; Baik, K.H. Effects of Partial Substitution of CeO_2 with M_2O_3 (M = Yb, Gd, Sm) on Electrical Degradation of Sc_2O_3 and CeO_2 Co-doped ZrO_2. *J. Korean Ceram. Soc.* **2016**, *53*, 500–505. [CrossRef]

21. Chong, F.D.; Tan, C.Y.; Singh, R.; Muchtar, A.; Somalu, M.R.; Ng, C.K.; Yap, B.K.; Teh, Y.C.; Tan, Y.M. Effect of manganese oxide on the sinterability of 8mol% yttria-stabilized zirconia. *Mater. Charact.* **2016**, *120*, 331–336. [CrossRef]

22. Lee, J.G.; Jeon, O.S.; Ryu, K.H.; Park, M.G.; Min, S.H.; Hyun, S.H.; Shul, Y.G. Effects of 8mol% yttria-stabilized zirconia with copper oxide on solid oxide fuel cell performance. *Ceram. Int.* **2015**, *41*, 7982–7988. [CrossRef]

23. Satardekar, P.; Montinaro, D.; Sglavo, V.M. Fe-doped YSZ electrolyte for the fabrication of metal supported-SOFC by co-sintering. *Ceram. Int.* **2015**, *41*, 9806–9812. [CrossRef]

24. López-Honorato, E.; Dessoliers, M.; Shapiro, I.P.; Wang, X.; Xiao, P. Improvements to the sintering of yttria-stabilized zirconia by the addition of Ni. *Ceram. Int.* **2012**, *38*, 6777–6782. [CrossRef]

25. Myung, J.-H.; Ko, H.J.; Park, H.-G.; Hwan, M.; Hyun, S.-H. Fabrication and characterization of planar-type SOFC unit cells using the tape-casting/lamination/co-firing method. *Int. J. Hydrogen Energy* **2012**, *37*, 498–504. [CrossRef]

26. Likhittaphon, S.; Pukkrueapun, T.; Seeharaj, P.; Wetwathana Hartley, U.; Laosiripojana, N.; Kim-Lohsoontorn, P. Effect of sintering additives on barium cerate based solid oxide electrolysis cell for syngas production from carbon dioxide and steam. *Fuel Process. Technol.* **2018**, *173*, 119–125. [CrossRef]

27. Barsoukov, E.; Mcdonald, J.R. *Impedance Spectroscopy Theory, Experiment, and Applications*; John Wiley & Sons: Hoboken, NJ, USA, 2005.

28. Vu, H.; Nguyen, D.; Fisher, J.G.; Moon, W.-H.; Bae, S.; Park, H.-G.; Park, B.-G. CuO-based sintering aids for low temperature sintering of $BaFe_{12}O_{19}$ ceramics. *J. Asian Ceram. Soc.* **2013**, *1*, 170–177. [CrossRef]

29. Liou, Y.-C.; Wu, C.-T.; Huang, Y.-L.; Chung, T.-C. Effect of CuO on $CaTiO_3$ perovskite ceramics prepared using a direct sintering process. *J. Nucl. Mater.* **2009**, *393*, 492–496. [CrossRef]

30. Amsif, M.; Marrero-López, D.; Ruiz-Morales, J.C.; Savvin, S.N.; Núñez, P. Effect of sintering aids on the conductivity of $BaCe_{0.9}Ln_{0.1}O_3-\delta$. *J. Power Sources* **2011**, *196*, 9154–9163. [CrossRef]

31. Liu, S.-S.; Li, H.; Xiao, W.-D. Sintering effect on crystallite size, hydrogen bond structure and morphology of the silane-derived silicon powders. *Powder Technol.* **2015**, *273*, 40–46. [CrossRef]

32. Presto, S.; Viviani, M. Effect of CuO on microstructure and conductivity of Y-doped $BaCeO_3$. *Solid State Ion.* **2016**, *295*, 111–116. [CrossRef]

33. Zhang, W.; Sun, C. Effects of CuO on the microstructure and electrochemical properties of garnet-type $Li_{6.3}La_3Zr_{1.65}W_{0.35}O_{12}$ solid electrolyte. *J. Phys. Chem. Solids* **2019**, *135*, 109080. [CrossRef]

34. Zhang, C.; Sunarso, J.; Zhu, Z.; Wang, S.; Liu, S. Enhanced oxygen permeability and electronic conductivity of $Ce_{0.8}Gd_{0.2}O_2-\delta$ membrane via the addition of sintering aids. *Solid State Ion.* **2017**, *310*, 121–128. [CrossRef]

35. Nicollet, C.; Waxin, J.; Dupeyron, T.; Flura, A.; Heintz, J.-M.; Ouweltjes, J.P.; Piccardo, P.; Rougier, A.; Grenier, J.-C.; Bassat, J.-M. Gadolinium doped ceria interlayers for Solid Oxide Fuel Cells cathodes: Enhanced reactivity with sintering aids (Li, Cu, Zn), and improved densification by infiltration. *J. Power Sources* **2017**, *372*, 157–165. [CrossRef]

36. Zhang, X.; Decès-Petit, C.; Yick, S.; Robertson, M.; Kesler, O.; Maric, R.; Ghosh, D. A study on sintering aids for $Sm_{0.2}Ce_{0.8}O_{1.9}$ electrolyte. *J. Power Sources* **2006**, *162*, 480–485. [CrossRef]

37. Choi, H.-J.; Na, Y.-H.; Kwak, M.; Kim, T.W.; Seo, D.-W.; Woo, S.-K.; Kim, S.-D. Development of solid oxide cells by co-sintering of GDC diffusion barriers with LSCF air electrode. *Ceram. Int.* **2017**, *43*, 13653–13660. [CrossRef]